DISTRIBUTION STATEMENT A. Approved for public release; distribution is unlimited.

New Approaches to the Parameterization of Gravity-Wave and Flow-Blocking Drag due to Unresolved Mesoscale Orography Guided by Mesoscale Model Predictability Research

Stephen D. Eckermann
Geospace Science & Technology Branch
Code 7631, Space Science Division
Naval Research Laboratory
Washington DC 20375
Phone: (202) 404-1299 Fax: (202) 404-7997 email: stephen.eckermann@nrl.navy.mil

Award Number: N0001411WX21220
http://geospace.nrl.navy.mil/gst/?content=section;code=7631

LONG-TERM GOALS

When surface flow impinges on orography with horizontal scales of ~1-500 km, a variety of mesoscale dynamical responses can result, including gravity waves, upstream blocking, flow splitting and lee vortices. These dynamics produce important drag forces on the larger scale atmosphere. Because global numerical weather and climate prediction (NWCP) models under-resolve orography at these scales, all credible NWCP systems must include parameterizations of these missing orographic mesoscale drag (OMD) forces. Recent evidence from mesoscale model simulations clearly indicates that OMD forces cannot be described as a purely deterministic response to upstream forcing, but instead can exhibit a range of values, time histories and states. Our long-term goals are (a) to build these new OMD dynamics delineated from mesoscale models into a new class of OMD parameterizations, (b) to embed those new parameterizations within Navy NWCP systems, and (c) to investigate whether improved time-mean OMD and new explicit OMD variability can improve NCWP skill in Navy global NWCP systems across a range of scales.

OBJECTIVES

The objective of this project is to develop a new class of subgrid-scale parameterizations of gravity-wave and flow-blocking drag due to flow incident upon unresolved mesoscale orography that (a) builds upon the existing OMD parameterization currently implemented in Navy NWCP models (Webster et al. 2003), but (b) modifies it's behavior in ways that both recognize and explicitly incorporate realistic distributions of possible OMD values that can arise for a given upstream flow environment, as deduced from fully nonlinear mesoscale model ensemble simulations.

APPROACH

Our approach involves a three-tiered research, development and transition (RD&T) strategy based around (a) first-principles mesoscale modeling of the fundamental nature and morphology of OMD dynamics, (b) OMD parameterization based on the results from (a), and (c) objective testing of these new OMD parameterizations in Navy NWCP models.

For tasks in (a) we leverage results from detailed suites of high-resolution simulations of orographic mesoscale flow dynamics from the Coupled Ocean-Atmosphere Mesoscale Prediction System (COAMPS®), both those from larger research projects at the Naval Research Laboratory (NRL) and a specific subset of companion simulations in this project specifically targeted to our OMD objectives. We analyze these mesoscale model fields to characterize the properties of OMD in various flow and orographic environments (both idealized and realistic). The resulting statistics are compiled as a function of time, mountain height (inverse surface Froude number) and obstacle aspect ratio, using the "regime diagram" approach that currently defines deterministic OMD responses in parameterizations (see Figure 1). This work delineates regions of this regime space that yield reproducible (deterministic) OMD and others that instead yield vacillating or even chaotic OMD. These new results in turn facilitate generalizations of the deterministic regime diagram responses in current OMD parameterizations to new hybrid responses that can vary, from constant deterministic OMD, to periodic/vacillating OMD, to purely stochastic and/or chaotic OMD, depending on their location in the regime space of Figure 1.

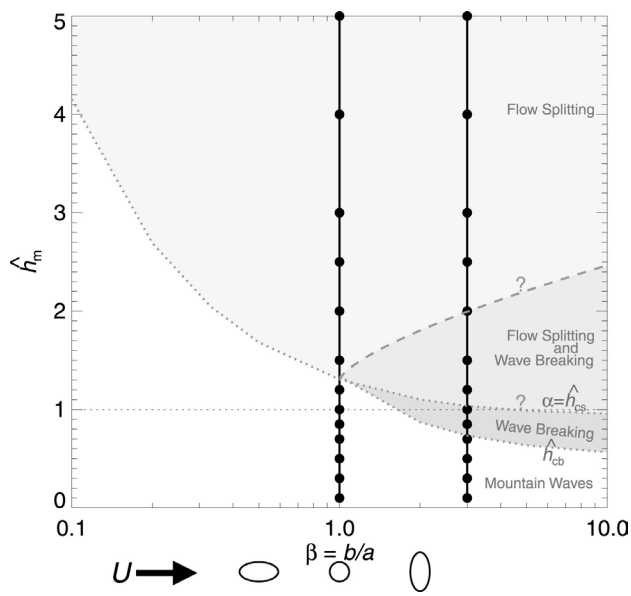

Figure 1. Regime diagram delineating OMD responses to uniform upstream flow of speed U and stability N, as a function of normalized obstacle height $\hat{h}_m = h_m N / U$ ***and obstacle aspect ratio β (after Eckermann et al. 2010).***

Tasks in category (b) focus on modifying the existing deterministic OMD scheme of Webster et al. (2003) in the Navy Global Environmental Model (NAVGEM) to include more realistic OMD properties and variability. Based on the existing literature (e.g., Doyle and Reynolds 2008; Eckermann et al. 2010), there appear to be (at least) two types of temporal OMD variability: (i) periodic vacillations due to cyclical buildup and breakdown of wavebreaking states, and (ii) quasi-chaotic vacillations due to complex internal sensitivities in the nonlinear mesoscale dynamics. We seek initial parameterizations of both types of response using explicitly stochastic methods, in which the range of temporal OMD variability is prescribed but the time history is random, thereby yielding realistic spread and variability in the time mean. For the orographic gravity-wave (OGW) component, we pursue the stochastic approach developed for multi-wave nonorographic gravity-wave drag (NGWD) by Eckermann (2011), and apply it to the orographic problem. Since multiwave methods are required

for accurate OGWD parameterization in three-dimensional flows across three-dimensional obstacles (e.g., Shutts 1995), we seek single-wave stochastic analogues for those applications based on the successful NGWD approach of Eckermann (2011). We also seek to use powerful new Hilbert transform methods based on the diagnostic Fourier-ray method described by Eckermann et al. (2010) for analyzing the gravity-wave content of mesoscale model output. In particular, we apply the method to quantify and parameterize for the first time the important process of three-dimensional geometrical spreading and its effects on wave amplitude growth with height and the transition to wave breaking and drag, a process currently omitted entirely from parameterizations. Since the total OMD across the obstacle must also be apportioned into OGW and orographic flow-blocking (OFB) contributions, we also seek stochastic parameterizations for the surface OFB component, based on (a) extending the simple analytical current calculations based on critical Froude numbers that locate the altitude of a dividing streamline, and (b) adapting the Webster et al. (2003) approach of heuristic fits to model-simulated OFB to incorporate realistic ranges of modeled variability within stochastic frameworks.

Tasks in category (c) implement the new OMD parameterizations in NAVGEM and assess performance, first in offline single column tests and ultimately in full forecast-assimilation experiments with results benchmarked using objective skill scores.

WORK COMPLETED

The following tasks were performed in this second year of work, building upon work completed in Year 1 of the project and documented in last year's report.

- We generalized our stochastic parameterization of nonorographic gravity wave drag (Eckermann 2011: see Year 1 report) to include newly separate extratropical and tropical source spectra (see Figure 2) to improve wave-forced tropical circulations.
- We performed additional COAMPS numerical experiments for studying OMD responses to idealized upstream flow as a function of normalized obstacle height and aspect ratio (Figure 1).
- We completed our numerical COAMPS and FR experiments exploring using HT FR techniques the parameter space of geometrical spreading (GS) effects on orographic GW amplitudes as a function of height (z), obstacle aspect ratio (β) and obstacle orientation angle (α).
- We generalized GW ray methods to develop a new ray density method for computing complete solutions to the wave action equation for three-dimensional GWs in arbitrary environments and validated the method in a pubished numerical study applied to an idealized model of convectively generated three-dimensional GWs (Broutman and Eckermann 2012).
- We conducted initial investigations into adding GS effects into OMD parameterizations based on new functional fits covering the full parameter space.

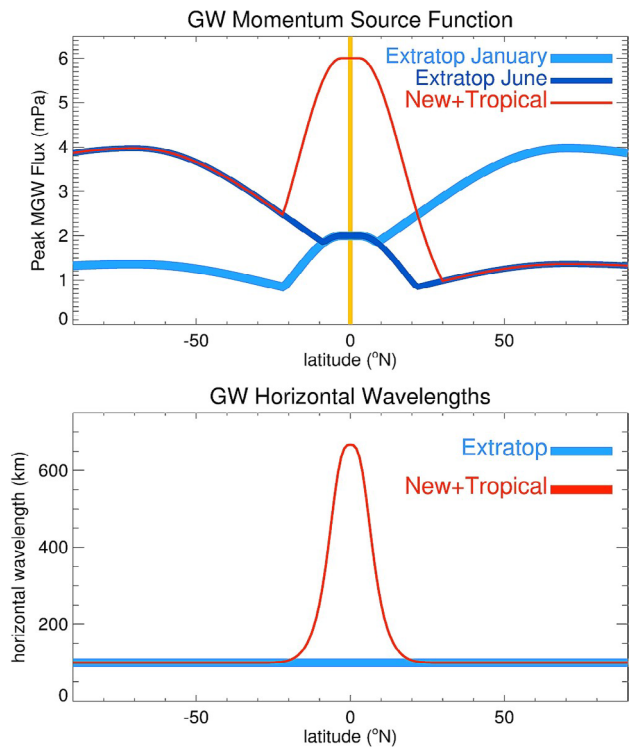

Figure 2. Plots of the wave source spectra for (top) total wave momentum (mPa) and (b) horizontal wavelength (km) as implemented this year in the stochastic gravity-wave drag parameterization of Eckermann (2011). Extratropical settings are shown in blue/purple, tropical settings in red.

RESULTS

We extended the Eckermann (2011) stochastic GW drag parameterization to contain newly separate extratropical and tropical source spectral characteristics, as shown in Figure 2. These choices were based to some extent on observed GW characteristics and physics. We tested and tuned these parameterized sources in single column experiments and then implemented and further tuned them in a high-altitude prototype of the Navy Operational Global Atmospheric Prediction System (NOGAPS). After reducing upper-level vertical diffusion, the new scheme produced for the first time a realistic semiannual oscillation (SAO) and quasi-biennial oscillation (QBO) of stratospheric equatorial winds in long-term (10-year) nature runs. The ability of these new schemes to generate and maintain tropical SAO and QBO circulations in Navy models for the first time is an important breakthrough, since these circulations will be critical to future seasonal prediction capabilities in NAVGEM. This work also validates the viability and stability of stochastic parameterization approaches to the gravity-wave drag problem generally in Navy models.

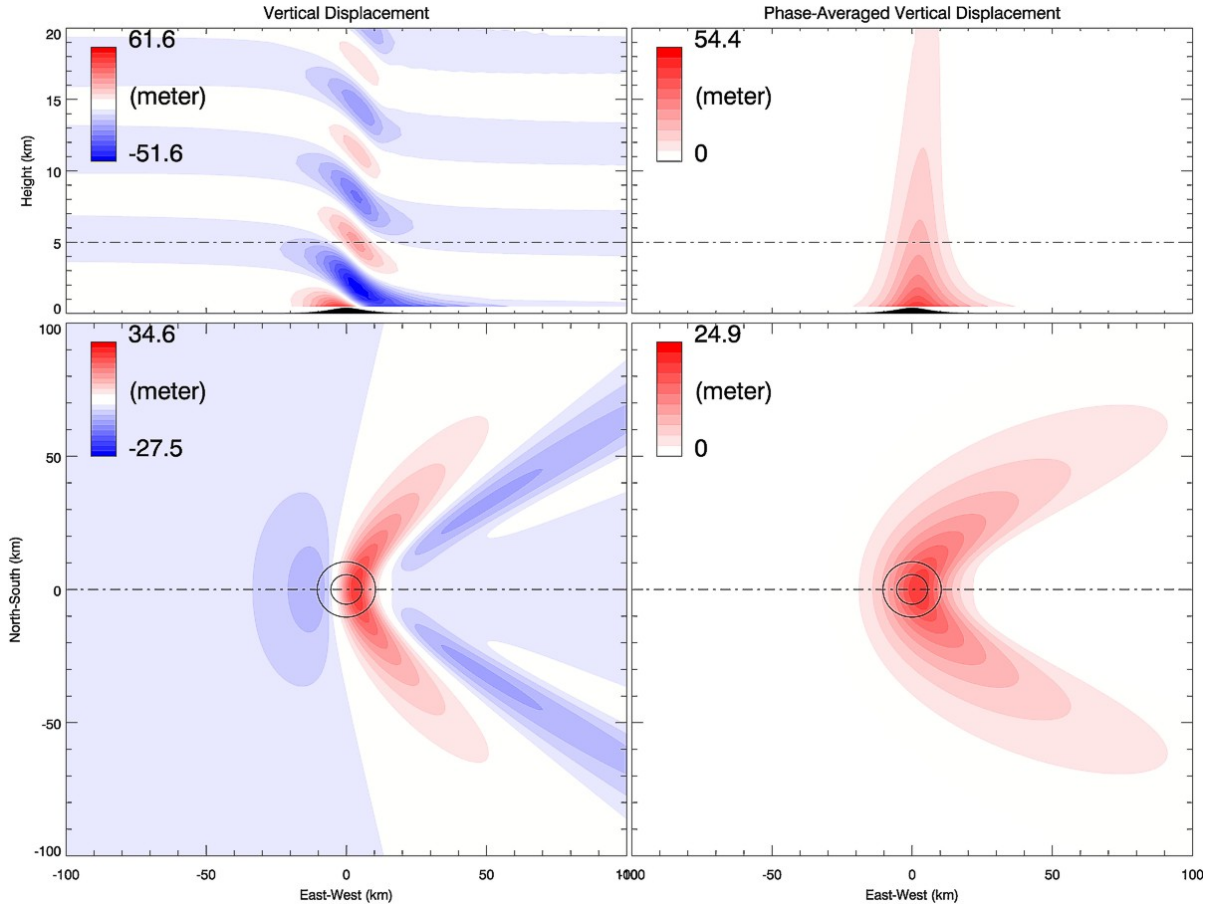

Figure 3. Illustration/validation of our Hilbert transform (HT) method of converting standard three-dimensional mountain wave solutions containing mixtures of amplitude (vertical displacement) and phase (left column) into corresponding solutions on the right for the peak (vertical displacement) amplitude only, with phase removed, which permit us to diagnose geometrical spreading effects on wave amplitudes with high accuracy for the first time.

In separate work, we applied our FR-based diagnostic Hilbert Transform (HT) method, tested in Year 1, to output fields from COAMPS and linear FR simulations of 3D orographic gravity waves to diagnose locations and values of peak wave amplitudes in the solutions. The HT method is described in greater detail by Eckermann et al. (2010). A simple illustration of the practical application of the HT technique for the current science problem is provided in Figure 3, which shows conventional mountain-wave solutions of the left containing the usual mixture of amplitude and phase, and corresponding solutions on the right after the complex FR coefficients of that solution have been combined using HT methods to remove phase from the solution and retain only peak amplitude. The plots on the right allow easy diagnosis of the horizontal and vertical locations of peak wave amplitudes in this, or indeed any other, three-dimensional stationary mountain wave solution.

We have utilized this capability to generate peak-amplitude fields like those on the right of Figure 3 for wave solutions radiated from a range of obstacle shapes, orientations and flow profiles spanning the fluid dynamics parameter space. In particular, we covered the β parameter space of wave regime reponses (see Figure 1) using a range of elliptical obstacle aspect ratios $\beta=b/a$, where b (a) is the length of the semimajor axis of the elliptical obstacle orthogonal (parallel) to the surface flow direction.

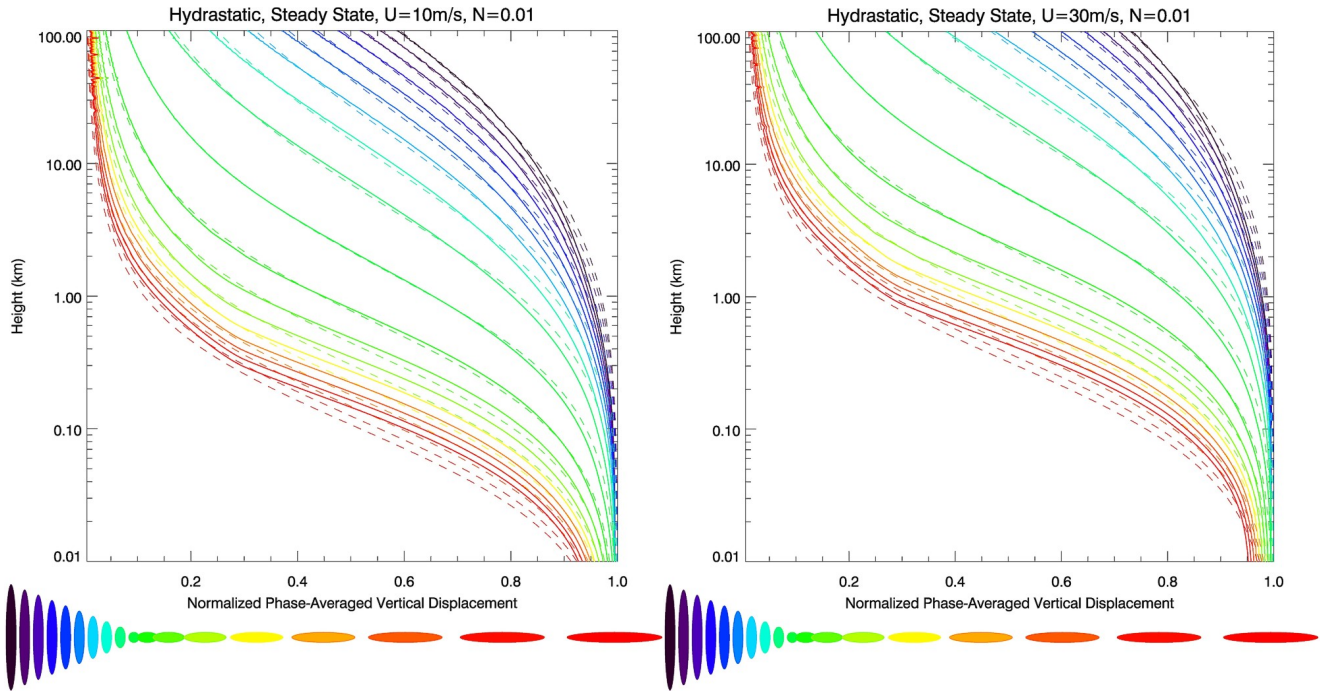

Figure 4. Variation with height of normalized peak vertical displacement amplitude for varying elliptical obstacle aspect ratios β, ranging from β=10 (black) to β=1 (green) to β=0.1 (red), as depicted with colored elliptical obstacle shapes beneath each panel. Results are shown for a constant N=0.01 s^{-1} and a constant eastward wind speed U of 10 m s^{-1} (left panel) and 30 m s^{-1} (right panel). The curves illustrate the large, first-order influence of three-dimensional geometrical in controlling wave amplitudes as these curves move away from the no-spreading limiting amplitude of unity at all heights. Results also show the strong sensitivity to β. Solid curves show results from numerical experiments, dotted curves show results from an analytical functional fit to these curves based on eq. (1) that is potentially useful for parameterization.

Figure 4 plots the height variation of the normalized vertical displacement amplitude of the mountain wave solution as β varies from 10 (black curves) to unity (green curves) and then through to 0.1 (red curves). The specific obstacle shape corresponding to the gradual change of β values in these experiments is depicted in color-coded form beneath each panel in Figure 4. The results show the familiar qualitative trend in geometrical spreading: that large β obstacles produce the smallest geometrical spreading, whereas axisymmetric obstacles (β=1) produce greater spreading due to three-dimensional ship-wave-like responses, whereas small β (β<<1) obstacles produce very large amounts of spreading due to large amounts of lateral GW dispersion. What is new here is the definitive quantification of the spreading effects on vertical wave amplitude evolution with height. Figure 4 shows that, even for axisymmetric obstacles, a proper treatment of geometrical spreading produces a wave amplitude at 10 km altitude that is a factor of 5 times weaker in local peak amplitude than the conventional parameterization solution that assumes that spreading effects are negligible (normalized amplitude of unity). Moreover, even large β obstacles reveal factor of two differences at 100 km due to spreading. Our work proves unambiguously that geometrical spreading is a first-order effect in diagnosing wave amplitude evolution and wave breaking in parameterizations.

The challenge is to come up with a conveniently cheap yet accurate fit of these bulk effects of spreading that is amenable to parameterization. Dotted curves in Figure 4 show corresponding fits to these solid curves, which, after experimentation, was based on the functional form

$$\eta(U,N,z,\beta) = \left[1 + G(\beta)\left\{(1 + Nz/U)^{1/2} - 1\right\}\right]^{-1} \qquad (1)$$

for the normalized GW peak amplitude η, where U is surface wind speed, N is buoyancy frequency, and z is altitude. Note the asymptotic range-dependent $z^{-1/2}$ tendency at large z in eq. (1) that comes as a limiting (far-field) idealized ray solution, as we demonstrated in a simpler context in Broutman and Eckermann (2012). Each curve was fitted to the function in eq. (1) using a least-squares procedure. This gives a range of fitted G values as a function of β. As shown in Figure 5, we were able to fit the variation G as a function of β closely using the functional form

$$G = e^{A}\beta^{-B} \quad \Rightarrow \quad \ln G = A - B\ln\beta \qquad (2)$$

We also investigated how the normalized peak amplitudes varied as a orientation angle α with respect to the surface flow direction was varied from 0° through 90°. The results are plotted in Figure 6 for the specific cases of rotating a β=2 obstacle progressively through 90° to become a β=½ obstacle. The normalized curves are shown on the left as solid curves from the numerical experiments. The broken curves show corresponding fits using the functional fits in eqs. (1) and (2), but now introducing a smooth variation with orientation angle α in fitted B coefficients as

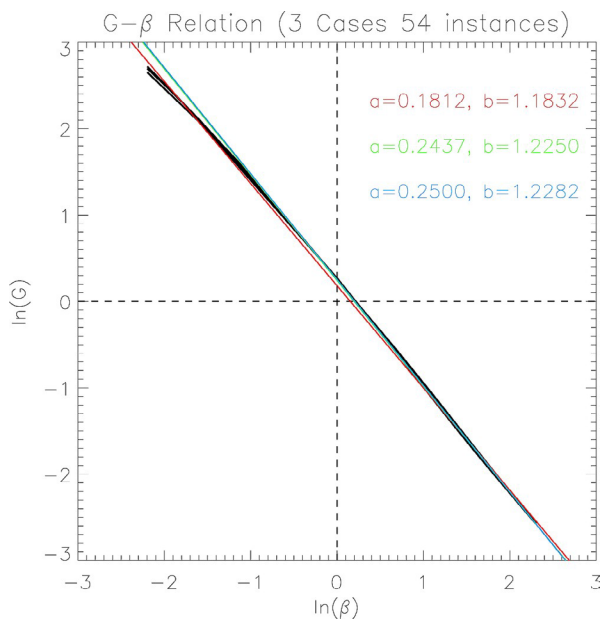

Figure 5. Variation of fitted G factors with β from numerical GW experiments and FR-based HT diagnosis of peak wave amplitudes in Figure 4. Note the linear fit on logarithmic axes which verifies a close fit to the functional form in eq. (2)

$$B(\alpha) = B(0)\cos\alpha + B(\pi/2)(1-\cos\alpha) \tag{3}$$

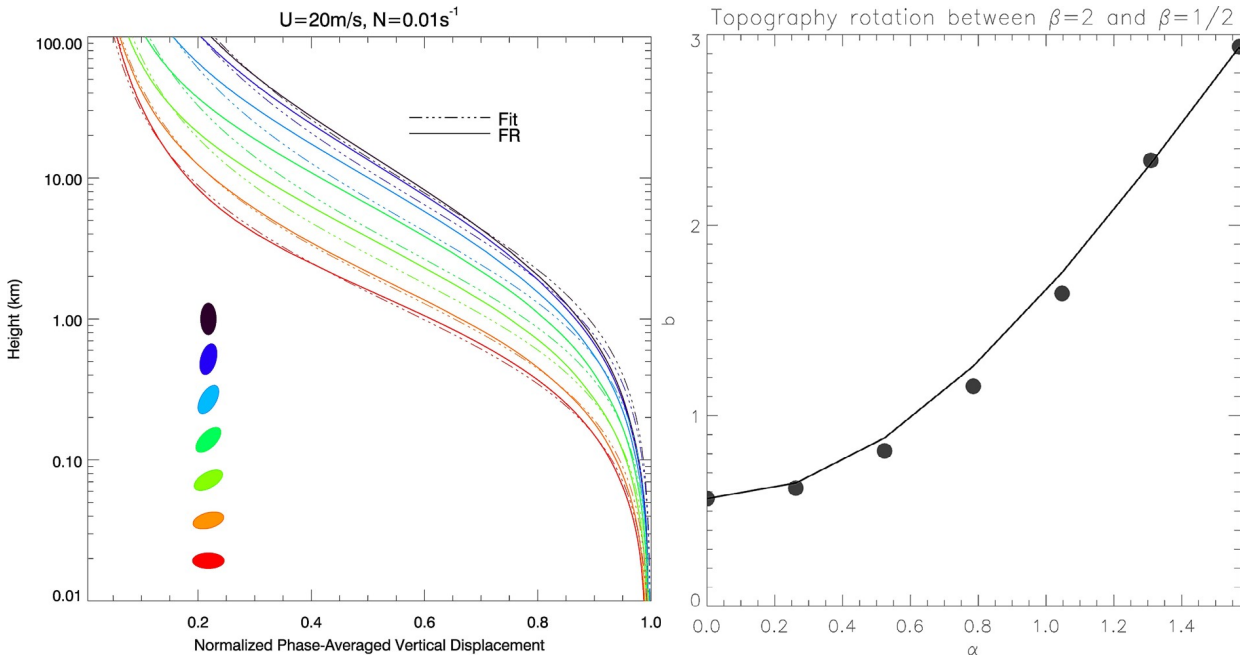

Figure 6. Left panel: Plots of variation of normalized vertical displacement peak amplitude for the β=2 obstacle (black) as it is progressively rotated by the angle α from 0 to π/4 (45°: green) and finally to π/2 (90°: red) yielding the β=1/2 obstacle simulation. Right panel: Solid curve shows corresponding fit of data (filled citcles) using eq. (3).

Such that, from the symmetry of the problem, $B(\pi/2) = 1/B(0)$. The data points versus α from the experiments are plotted as filled circles in the right panel of Figure 6, with the fit from eq. (3) shown as the solid curve, revealing again a close fit that is again amenable to a computationally efficient parameterization of the dominant effects.

We have commenced preliminary tests to include these new parameterization fits plus stochastic OMD ranges delineated in Year 1 into the OMD parameterization of Webster et al. (2003) currently implemented in both NOGAPS and the NAVGEM prototype. This work is in its preliminary stages and so our Year 3 work will focus on fuller implementation of these GS and OMD results and detailed tests of the new parameterization performance in Navy global models, as well as publishing the new results summarized in Figures 2-5 in the peer-reviewed scientific literature.

IMPACT/APPLICATIONS

This project focused on new classes of OMD parameterization for weather and climate models generally, and for NAVGEM specifically. The parameterization of unresolved OMD is one of the more important parameterizations in weather and climate models, required for credible and accurate reproductions of mean sea-level pressure distributions in the Arctic, closure of lower stratospheric wind jets, and reversals of winds above the extratropical winter stratopause. The improved

parameterizations of OMD from this work should therefore result ultimately in improved prediction capabilities of weather and climate prediction models that incorporate the new schemes.

TRANSITIONS

We transitioned the latest version of the "team scheme" GWD code of Eckermann (2011) with tuned tropical and extratropical GW sources into the NOGAPS R&D prototype with Advanced-Level Physics and High-Altitude (ALPHA) as well as into a high-altitude developmental (dev) version of NAVGEM.

RELATED PROJECTS

Doyle, J. D., and S. D. Eckermann, *The Boundary Paradox*, NRL 6.1 Accelerated Research Initiative, 1 October 2010-30 September 2015.

REFERENCES

Doyle, J. D. and C. A. Reynolds (2008), Implications of regime transitions for mountain-wave-breaking predictability. Mon. Wea. Rev., 136, 5211–5223.

Eckermann, S. D. (2011), Explicitly stochastic parameterization of nonorographic gravity-wave drag, J. Atmos. Sci., 68, 1749-1765.

Eckermann, S. D., J. Lindeman, D. Broutman, J. Ma and Z. Boybeyi (2010), Momentum fluxes of gravity waves generated by variable Froude number flow over three-dimensional obstacles, J. Atmos. Sci., 67, 2260-2278.

Shutts, G.J. (1995), Gravity-wave drag parametrization over complex terrain: The effect of critical-level absorption in directional wind-shear. Quart. J. Roy. Meteor. Soc., 121, 1005-1021.

Webster, S., A. R. Brown, D. R. Cameron, and C. P. Jones (2003), Improvements to the representation of orography in the Met Office Unified Model. Quart. J. Roy. Meteor. Soc., 129, 1989–2010.

PUBLICATIONS

Broutman, D., and S. D. Eckermann (2012), Analysis of a ray-tracing model for gravity waves generated by tropospheric convection, J. Geophys. Res., 117, D05132, doi:10.1029/2011JD016975.

Eckermann, S. D. (2011), Explicitly stochastic parameterization of nonorographic gravity-wave drag, J. Atmos. Sci., 68, 1749-1765.